

Identification of potential inhibitors for Sterol C-24 reductase of *Leishmania donovani* through virtual screening of natural compounds

FAZLUR RAHMAN^{1, #}; SHAMS TABREZ^{1, #}; RAHAT ALI¹; SAJJADUL KADIR AKAND¹; MOHAMMED A. ALAIDAROUS^{2, 3}; MOHAMMED ALSAWEED²; BADER MOHAMMED ALSHEHRI²; SAEED BANAWAS^{2, 3}; ABDUR RUB^{1, *}; ABDUL AZIZ BIN DUKHYIL^{2, *}

¹ Infection and Immunity Laboratory (414), Department of Biotechnology, Jamia Millia Islamia-A Central University, New Delhi, 110025, India

² Department of Medical Laboratory Sciences, College of Applied Medical Sciences, Majmaah University, Al Majmaah, 11952, Saudi Arabia

³ Health and Basic Sciences Research Center, Majmaah University, Al Majmaah, 11952, Saudi Arabia

Key words: Leishmania, Gingerol, Sterol C-24 reductase, Molecular docking, ROS

Abstract: Leishmaniasis is a vector-borne parasitic neglected tropical disease caused by a group of about 30 different species of the genus *Leishmania*. It is transmitted by the bite of female phlebotomies sand fly. Three main clinical manifestations of leishmaniasis include cutaneous, visceral, and mucocutaneous leishmaniasis. Visceral leishmaniasis (VL) caused by *Leishmania donovani*, is an infection of reticuloendothelial system and fatal if untreated. Cholesterol, a sterol that is prominent in the mammalian cell membranes whereas stigmasterol and ergosterol are more prevalent in plants, yeast, and protozoa, respectively. Ergosterols which is absent in human being, is an important constituent of parasite membrane. Sterol C-24 reductase (*LdSR*) enzyme catalyzes the final step in the ergosterol biosynthesis pathway. The inhibition of biosynthesis of ergosterol may lead to decreased cell viability and growth. Here, we performed the molecular docking-based virtual screening of a library of natural ligands against *LdSR* to identify a potential inhibitor to fight leishmaniasis. Capsaicin, prenyletin, flavan-3-ol, resveratrol, and gingerol showed the top binding affinity towards *LdSR*. Based upon ADME properties and bioactivity score, gingerol showed the best lead-likeness and drug-likeness properties. Hence, we further annotated its leishmanicidal properties. We found that gingerol inhibited the growth and proliferation of promastigotes as well as intra-macrophagic amastigotes. Gingerol exerted its antileishmanial action through the induction of reactive oxygen species (ROS) in concentration-dependent manner. Gingerol induced ROS led to apoptosis. Overall, this study described that gingerol would act as possible inhibitor to *LdSR*.

Introduction

Leishmaniasis is a vector-borne parasitic neglected tropical disease caused by a group of about 30 different species of the genus *Leishmania*. It is transmitted by the bite of female phlebotomies sand fly and is not contagious (Burza *et al.*, 2018; Ghorbani and Farhoudi, 2018). An infected animal or human, bitten by a sandfly first infects the sandfly which is followed by the *Leishmania* parasite multiplication in the gut of the sandfly and becomes infective in 8–20 days. The parasites are passed on to an uninfected host when the sandfly bites (Desjeux, 2004). Three main clinical

manifestations of leishmaniasis include cutaneous, mucocutaneous, and visceral leishmaniasis (VL). Cutaneous leishmaniasis (CL) is the most common form worldwide which is caused by *Leishmania major* and *Leishmania tropica* in the Middle East and Central Asia and *Leishmania braziliensis* complex and *Leishmania mexicana* in America which usually cause ulcers on the skin (Elmahallawy *et al.*, 2014). VL (also known as the kala-azar disease) caused by *Leishmania infantum*, *Leishmania chagasi*, and *Leishmania donovani* complexes reflects dissemination of *Leishmania* parasites throughout the reticuloendothelial system and fatal if untreated (Aronson *et al.*, 2017; Ghorbani and Farhoudi, 2018). While mucocutaneous leishmaniasis is rare and includes lesions that can lead to the partial or total destruction of the mucous membranes of the mouth, nose, throat cavities, and surrounding tissues (Goto and Lauletta Lindoso, 2012). Around 1.5–2 million new cases of leishmaniasis are reported each year with 350 million people

*Address correspondence to: Abdur Rub, arub@jmi.ac.in; Abdul Aziz Bin Dukhyil, a.dukhyil@mu.edu.sa

#These authors contributed equally to this work

Received: 17 March 2021; Accepted: 25 April 2021

Doi: 10.32604/biocell.2021.016682

www.techscience.com/journal/biocell



This work is licensed under a Creative Commons Attribution 4.0 International License, which permits unrestricted use, distribution, and reproduction in any medium, provided the original work is properly cited.

at risk of acquiring the disease and leading to 70000 deaths (Torres-Guerrero *et al.*, 2017). With its major reservoir in developing countries mostly India, Bangladesh, and Nepal contributing to more than 50% of all the global cases, show a very strong link with poverty (Burza *et al.*, 2018). Within endemic areas, increased infection risk is mediated through poor housing conditions and environmental sanitation, lack of personal protective measures, and economically driven migration and employment that bring non-immune hosts into contact with infected sand flies (Ghorbani and Farhoudi, 2018). The factors that mainly determine the morbidity and mortality rate in the region are the genetic background of the population, geographical distribution, and sanitary conditions (Haftom *et al.*, 2020).

Sterols present in the cell membranes are primarily essential for the integrity and function of the membrane and helps in maintaining the fluidity, permeability, and activity of the membrane-bound proteins (He *et al.*, 2003). Cholesterol is a sterol that is prominent in the mammalian cell membranes whereas stigmasterol and ergosterol are more prevalent in plants, yeast, and protozoa, respectively. Ergosterols present in the membrane of *leishmania* parasites serve as good drug targets as mammalian hosts are devoid of ergosterol (Mccall *et al.*, 2015). *LdSR* enzyme catalyzes ergostetraenol to ergosterol, the final step in the ergosterol biosynthesis pathway. The absence of this enzyme is associated with a lack of ergosterol and leads to the accumulation of its substrate, ergosta-5, 7, 22, 24(28)-tetraen-3 β -ol (Gilk *et al.*, 2010). Studies have suggested that the inhibition of biosynthesis of ergosterol can lead to decreased cell viability (Mathur *et al.*, 2015). Presently, there is no universally accepted drug or vaccine available for leishmaniasis in humans. An antifungal drug, Amphotericin B which is used currently works primarily by binding to ergosterol present in the cell membranes of parasites leading to its instability and subsequently pore formation which increases the permeability of the membrane and kills the parasite. But the use of amphotericin B is very limited due to high toxicity and adverse side effects: chills, high fever, and renal failures. Another drug, Miltefosine is an oral medication that is used to treat leishmaniasis is anti-tumorous and causes apoptotic events in parasites for its killing. But it is associated with high teratogenicity and gastro-intestinal toxicity (Tiwari *et al.*, 2018). Natural bioactive compounds of food have a long history of treating illnesses such as fever, diarrhea, inflammation, and many chronic diseases. Bioactive compounds such as faltarinol and faltarindiol are abundant polyacetylenes present in carrots show anti-inflammatory activity by suppressing NF κ B. Polyphenols derived from Congee have shown promising results in promoting bone health (Teodoro, 2019). Structure-based virtual high-throughput screening has been categorized as an advanced computational approach being used for the identification of lead and their optimization for drug discovery programs by screening ligand libraries (Rollinger *et al.*, 2008).

In our study, we have used the molecular docking approach to find a lead molecule against the *LdSR* enzyme by screening a natural ligands library prepared based on a wide literature search. Different approaches such as

template-based 3D structure modelling in association with virtual screening, minimum binding energy, and other related parameter-based analysis (Cheng *et al.*, 2012) have been employed to evaluate the affinity of ligands by functional inhibition and chemical targeting our selected macromolecule to find a potent leishmanicidal drug molecule.

Materials and Methods

Materials

The chemicals used in the study were procured from well-known standard companies. M199 media, RPMI1640 media, Fetal bovine serum (FBS), penicillin-streptomycin (pen-strip) antibiotic, trypan blue, were procured from Gibco-Thermo-Fisher, Waltham, MA, USA. Phorbol-3myristate acetate (PMA), was procured from peprotech. Methylthiazolyldiphenyl-tetrazolium bromide (MTT) was purchased from Merck & Co., Inc., Kenilworth, NJ, USA. Formaldehyde, GIEMSA stain, propidium iodide were purchased from Thermo-Fisher, Waltham, MA, USA. Annexin-FITC was from BD Biosciences, San Jose, CA. Gingerol was purchased from ChemScene, India. All the other chemicals were purchased from Merck & Co., Inc., Kenilworth, NJ, USA, unless otherwise stated.

Ligand library preparation, structure modelling and molecular docking

The 3D structure of the ligands was downloaded from the PubChem database in sdf format (Kim, 2016). Open Babel GUI is a freely available software, was used to change the atomic coordinates to pdbqt, and energy was minimized by Universal Force Field (uff) (O'boyle *et al.*, 2011; Rappé *et al.*, 1992). Our lab had homology modelled the 3D structure of the *LdSR* of *L. donovani* due to non-availability of its crystal structure (Tabrez *et al.*, 2021). Discovery studio and CASTp server were operated for predicting the binding pocket residues of *LdSR* by keeping the value of the probe radius (1.4) at default (Tabrez *et al.*, 2021; Tian *et al.*, 2018). For the molecular docking study, we have used PyRx to predict the significant binding affinity and to evaluate the finest binding mode (Dallakyan and Olson, 2015). OpenBabel in PyRx was used to change the atomic coordinates of the *LdSR* enzyme to pdbqt files for docking studies. The minimum binding energy and the detailed interactions comprising of van der Waals interactions, conventional hydrogen bonds, pi-anion, alkyl, and pi-alkyl, etc. by Discovery Studio were explored for the significant binding affinity and pose (Rahman *et al.*, 2021). The inhibition constant (K_i) was calculated as per the previous publication (Rahman *et al.*, 2021).

Parasite and cell culture

Leishmania donovani cultures (MHOM/IN/83/AG83) were maintained in M199 media pH 7.4, supplemented with 10% heat-inactivated fetal bovine serum (FBS), and 1% penicillin-streptomycin antibiotic at 22°C. The parasites were regularly passaged at the interval of 4 days after adjusting the inoculum density of 2×10^6 parasites/mL. THP-1 cell line (Human leukemia cells) was cultured in RPMI-1640 media with 10% FBS and 1% penicillin-streptomycin antibiotic and

maintained at 37°C and 5% CO₂. The stock concentration of the compound was prepared in blank M199 media. THP-1 monocytic cells were stimulated with 20 ng/ml of phorbol 3-myristate acetate (PMA) for differentiation to macrophages.

Anti-promastigote assay

2 × 10⁶ cells/mL of promastigote phase parasites were incubated without or with a two-fold serial dilution of gingerol for 48 h at 22°C. After 48 h of incubation at 22°C, the parasites were fixed in 1% paraformaldehyde and enumerated using a hemocytometer. The percentage inhibition was calculated, by considering negative control as 100%. Mean percentage of viability was calculated as per the labs established protocol (Tabrez *et al.*, 2021). The 50% inhibitory concentration (IC₅₀) (concentration that decreased the growth of the parasite by 50%) was determined by extrapolating the graph of % viability versus concentrations of the compound.

Cell cytotoxicity assay

To determine the adverse effect of gingerol, differentiated THP-1 cells were incubated with a two-fold serial dilution of gingerol up to 1000 µg/mL for 24 h at 37°C in a humidified 5% CO₂ incubator. After 24 h of incubation, the media was removed and further incubated with 50 µM of MTT for 3–4 h in a CO₂ incubator followed by the resuspension of formed formazan in DMSO. The absorbance of the samples was measured at 570 nm in an ELISA plate reader and percentage viability was calculated.

Anti-intramacrophagic amastigotes assay

0.5 × 10⁶ THP-1 cells were seeded on the coverslip in a six-well plate and stimulated with PMA, after proper differentiation to macrophages, were infected with 3rd to 4th day virulent promastigotes in the ratio of 1:10 (macrophage to *L. donovani*) for 24 h. The non-phagocytosed parasites were washed with 1 × PBS and the infected macrophages were incubated with different concentrations of the gingerol for 24 h. The coverslip was washed thrice with 1 × PBS, fixed with chilled methanol, and stained by using modified Giemsa stain for amastigote microscopic evaluation. About 100 macrophages were counted from different focus to evaluate the effect of the treatment on the macrophagic parasite burden.

ROS analysis in parasites

To evaluate the outcome of gingerol on ROS generation in *L. donovani*, 2,7-dichloro dihydro fluorescein diacetate (H₂DCFDA) dye was utilized. After washing three times with 1 × PBS, the treated parasites were incubated in 10 µM of H₂DCFDA for 20 min in the dark. BD FACS ARIA III flow cytometer was used to capture the signal as fluorescence for each sample. The data were recorded and represented as histograms.

Annexin V and PI staining

For the apoptotic assay, treated and untreated parasites were centrifuged at 3000 rpm for 5 min, and washed thrice with 1 × PBS. Finally, the pellet was resuspended in 100 µL of 1 × binding buffer (10 mM HEPES (pH 7.4), 140 mM NaCl and 2.5 mM CaCl₂) containing 5 µL of annexin-FITC and 5 µL of propidium iodide for 25 min in the dark at room

temperature followed by adding 400 µL of binding buffer before analysis. The samples were analyzed through BD FACSaria III Cell Sorter.

Statistical analysis

All the experiments were performed in triplicate and the results represented are the mean of the triplicate with SD. Statistical analysis was performed using Graph pad prism 7.0 software and a *P*-value of less than 0.05 (*P* ≤ 0.05) was considered significant. The statistical significance was calculated using *t*-tests.

Results

Molecular docking based virtual screening of ligands library showed the best interaction of LdSR with gingerol

Based on a wide literature search, the natural ligand-based library was prepared consisting of antimalarial, antibacterial, antiviral, and antifungal properties (Tab. 1). The ligand library comprising natural compounds was virtually screened against the homology based modelled structure of LdSR (Suppl. Fig. S1.), their binding energies and pKipred were predicted (Tab. 2). Out of these, gingerol was found to have best affinity and binding energy of –6.8 Kcal/mol and settled in the catalytic pocket of LdSR (Fig. 1A, Tab. 2). The five conventional intramolecular hydrogen bonds showed important interactions between gingerol and the Tyr294, Trp367(2), His428, and Arg464 residues of LdSR ranging from 2.2 Å to 2.6 Å (Fig. 1B, Tab. 3). Furthermore, gingerol was found to interact strongly with other residues of the catalytic pocket of LdSR. The pi-anion bond was formed by the residue Asp432 of LdSR with the ring present in the gingerol. Further, eight alkyl and pi-alkyl bonds formed by Trp259, Leu262, Tyr294(2), Val295, Tyr332(2), and Trp367 aid in stabilizing the LdSR-gingerol complex (Fig. 1C, Tab. 3). We further evaluated their lead likeness and enzyme inhibition activities by exploring ADME properties (Daina *et al.*, 2017) and bioactivity score (<https://www.molinspiration.com/cgi-bin/properties>), we found that gingerol had significant drug-likeness properties (Tab. 4). The interaction of gingerol within the deep cavity of LdSR may hinder the substrate accessibility and consequently, may have an inhibitory potential.

Anti-promastigote evaluation of gingerol and IC₅₀ value determination

After gaining the insight from *in silico* results regarding *L. donovani*-sterol pathway inhibitory potential of gingerol, we further tried to evaluate its antileishmanial potential *in vitro*. It was evaluated against the *L. donovani* promastigotes by enumerating the viable parasites left after 48 h of incubation with gingerol. (0.00 to 1000 µM), demonstrated a concentration-dependent killing of the parasites (Fig. 2A). The IC₅₀ value was determined by extrapolating the line graph of % viability versus dose concentration and it was found to be 239.5 ± 19.26 µM (Fig. 2B).

Cytotoxicity of gingerol on mammalian macrophages

To ensure the safety limit of gingerol, differentiated THP-1 cells were incubated at its different concentrations and

TABLE 1

Natural ligand library of antimicrobial compounds

S. No.	Ligands (Natural compounds)	Activity	References
1.	Acetylugenol	Against <i>Proteus</i> sp., <i>Salmonella typhi</i> , <i>Staphylococcus aureus</i> , and <i>Streptococcus pneumonia</i>	(Abdulhamid <i>et al.</i> , 2021)
2.	Prenyletin	Against <i>T. rubrum</i> ; <i>T. mentagrophytes</i>	(de Andrade Monteiro and Ribeiro Alves Dos Santos, 2019)
3.	Lactacystin	Against <i>Mycobacterium tuberculosis</i>	(Maiolini <i>et al.</i> , 2020)
4.	Resveratrol	Against MERS-CoV infection Against Influenza A virus Against <i>Mycobacterium tuberculosis</i>	(Lin <i>et al.</i> , 2017; Maiolini <i>et al.</i> , 2020; Palamara <i>et al.</i> , 2005)
5.	Flavan-3-ol	Against <i>Candida</i>	(de Andrade Monteiro and Ribeiro Alves Dos Santos, 2019)
6.	Capsaicin	Antibacterial	(Cichewicz and Thorpe, 1996; Jones Jr, and Luchsinger, 1986)
7.	Lawsone	Antifungal	(Al-Snafi, 2019)
8.	Gingerol	Against <i>M. tuberculosis</i>	(Bhaskar <i>et al.</i> , 2020)
9.	caffeic acid	Against Viruses, helminths	(Wild, 1994)
10.	Gigantol	Antimalarial, antiviral	(Simmler <i>et al.</i> , 2010)
11.	Thymol	Against Viruses, bacteria, Fungi	(Cowan, 1999)
12.	Eugenol	Bacteriostatic against both fungi and bacteria	(Cowan, 1999; Duke, 1987)
13.	Allicin	Against <i>Candida albicans</i> aspergillosis	(Dai <i>et al.</i> , 2020; Khodavandi <i>et al.</i> , 2011)
14.	Chavicol	Against <i>C.elegans</i>	(Zhou <i>et al.</i> , 2012)

TABLE 2

Molecular docking interaction of natural compounds with LdSR of *L. donovani*

S. No.	Ligands	Binding energy (Kcal/mol)	p Ki _{pred} (μM)
1.	Capsaicin	-7.0	5.14
2.	Prenyletin	-7.0	5.14
3.	Flavan-3-ol	-6.9	5.07
4.	Resveratrol	-6.9	5.07
5.	Gingerol	-6.8	5.00
6.	Lawsone	-6.7	4.93
7.	caffeic acid	-6.7	4.93
8.	Gigantol	-6.7	4.93
9.	Lactacystin	-6.6	4.86
10.	Acetylugenol	-6.6	4.86
11.	Eugenol	-6.0	4.41
12.	Thymol	-5.7	4.20
13.	Chavicol	-5.6	4.12
14.	Allicin	-3.9	2.87

Abbreviations: pKi-negative decimal logarithm of inhibition constant; pred-predicted.

cytotoxicity was evaluated. There was no significant adverse effect up to 250 μM, while at the concentration 500 and 1000 μM, it was found toxic (Fig. 2C.). Finally, its CC₅₀ was calculated as 401.30 + 47.07 μM.

Cytotoxicity of gingerol on mammalian macrophages

To ensure the safety limit of gingerol, differentiated THP-1 cells were incubated at its different concentrations and cytotoxicity was evaluated.

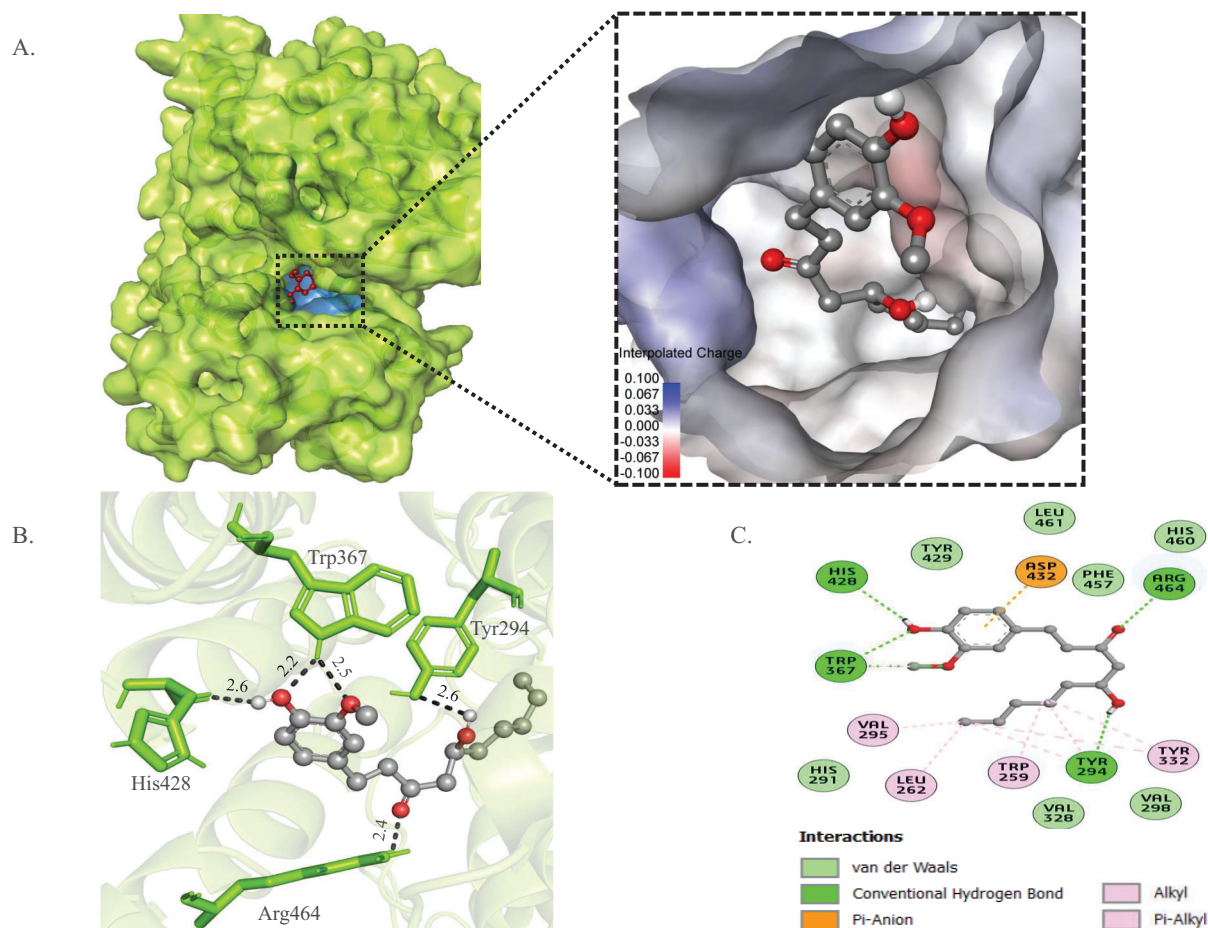


FIGURE 1. *In silico* analysis of the binding pattern of gingerol with *LdSR*. (A) The cartoon-surface representation and surface electrostatic potential of *LdSR* with gingerol after docking blocked the catalytic center. (B) 3D interactions of gingerol with the important residues of *LdSR*. (C) 2D plot of interaction of *LdSR* with gingerol.

TABLE 3

List of non-covalent interactions of gingerol with *LdSR* residues

S. No.	Interaction type	No. of interactions	Participating residues
1.	Hydrogen bonds	5	Tyr294, Trp367(2), His428, Arg464
2.	van der Waals	7	His291, Val298, Val328, Tyr429, Phe457, His460, Leu461
3.	Pi-anion	1	Asp432
4.	Alkyl & Pi-alkyl	8	Trp259, Leu262, Tyr294(2), Val295, Tyr332(2), Trp367

TABLE 4

ADME properties of the top natural compounds evaluated by Swiss-ADME and Bioactivity prediction by Molinspiration

S. No.	Compounds	Physicochemical properties					Lipophilicity (≤ 5)	Water solubility	Pharmacokinetics		Druglikeness (Lipinski, Ghose, Veber, Egan, Muegge)	Medicinal chemistry-Leadlikeness (Number of violations)	Bioactivity score (Enzyme inhibitor >0)
		M.W. (g/mol)	N.R.B., (≤ 10)	H.B.A., (≤ 10)	H.B.D., (≤ 5)	TPSA (\AA^2) (≤ 140)			GIA	BBB permeant			
1.	Capsaicin	305.41	10	3	2	58.56	3.15	Soluble	High	Yes	All yes	No (2)	0.07
2.	Prenyletin	246.26	3	4	1	59.67	2.80	Soluble	High	Yes	All yes	No (1)	0.09
3.	Flavan-3-ol	226.27	1	2	1	29.46	2.52	Soluble	High	Yes	All yes	No (1)	0.30
4.	Resveratrol	228.24	2	3	3	60.69	1.71	Soluble	High	Yes	All yes	No (1)	0.02
5.	Gingerol	294.39	10	4	2	66.76	3.48	Soluble	High	Yes	All yes	No (1)	0.38

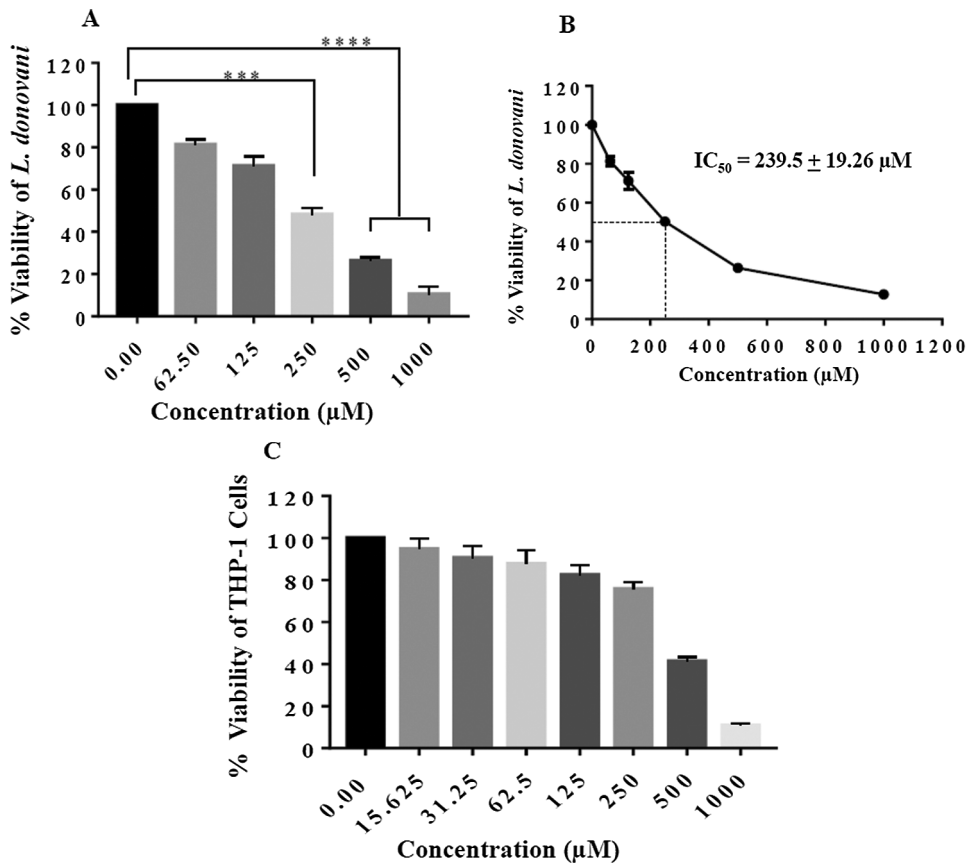


FIGURE 2. Anti-promastigote and cytotoxicity assay of gingerol. (A) Logarithmic phase, *L. donovani* promastigotes (2×10^6 parasites per ml), were treated with increasing concentration of gingerol, a dose respond was observed with increasing concentration. (B) % viability ascertained upon incubation of promastigotes for 48 h for IC_{50} determination. Each point or bar corresponds to the mean \pm SE. (C) Cytotoxicity of gingerol on THP-1 differentiated macrophages was studied and CC_{50} value determined as per the mentioned protocol. Each point corresponds to the mean \pm SE of triplicate samples. **** $P < 0.0001$; *** $P < 0.0002$.

Effects of gingerol against intracellular amastigotes

The antileishmanial potential of gingerol was further analyzed on internalized parasites inside macrophages upon treatment through Giemsa staining. Our results showed a concentration-dependent response of gingerol (0.00–250 μ M) on amastigote number. At the highest dose of 250 μ M of gingerol, there was significant reduction in the parasite count (Fig. 3A) with an IC_{50} value of $246.90 \pm 17.78 \mu$ M (Fig. 3B). Representative images of infected macrophages of different treatments were also taken better understanding (Fig. 3C).

Gingerol induced pro-oxidant activity in *L. donovani* promastigotes

Gingerol-treated promastigotes were analyzed for the oxidative status by using H2DCFDA dye. The intracellular ROS generated inside the parasite oxidizes H2DCFDA and produces a green-fluorescent signal. The green-fluorescent signal indicates oxidative stress condition. Hence, the amount of fluorescent signal is directly proportional to the level of ROS generation. An increase in concentration-dependent ROS generation was observed at 125 μ M and 250 μ M concentrations of gingerol. 51.3% of parasites were found ROS positive at 125 μ M concentration (Figs. 4A–4B). Additionally, 77.9% of parasites were observed ROS positive at 250 μ M concentration (Figs. 4A–4B). These data advocated the pro-oxidant effects of gingerol on *L. donovani* promastigotes.

Gingerol induced apoptosis in *L. donovani* promastigote

The translocation of phosphatidylserine (PS) from the inner to the outer leaflet (extracellular side) of the plasma membrane is a biomarker of apoptosis. Annexin V is a

cellular protein in the annexin group that is commonly used to detect apoptotic cells due to its ability to bind with phosphatidylserine. Annexin V is conjugated with a fluorescent dye, fluorescein isothiocyanate (FITC) to allow fluorescent detection of annexin V bound to apoptotic cells and quantitative determination through flow cytometry. Another commonly used non-permeable and red-fluorescent dye, Propidium iodide (PI) selectively enters inside necrotic cells and intercalates between DNA. At 125 μ M gingerol treatment 68.8% of the parasites' population were in early apoptosis and 27.5% were in late apoptosis (Figs. 5A–5B). As the concentration of gingerol was increased to 250 μ M, the population in the early apoptotic stage was declined from 68.8% to 52.2% while the parasites in the late apoptosis were increased from 27.5% to 44.9% (Figs. 5A–5B). This data suggested that the parasites experienced a concentration-dependent apoptosis on gingerol treatment.

Discussion

Molecular docking scrutiny was done to gain an insight into the interactions of the ligand with *LdSR* to actuate their binding affinity, bound confirmations, and binding energy of the possible interacting residues. Molecular docking of the ligand's library with *LdSR* had shown significant binding energies (Tab. 2). The top five ligands were selected based upon binding energy, hydrogen bonds under 3.5 Å, and hydrophobic bonds under 5.0 Å. Capsaicin, prenyletin, flavan-3-ol, resveratrol, and gingerol were found to have a significant binding energy of -7.0 kcal/mol, -7.0 kcal/mol, -6.9 kcal/mol, -6.9 kcal/mol, and -6.8 kcal/mol with *LdSR*,

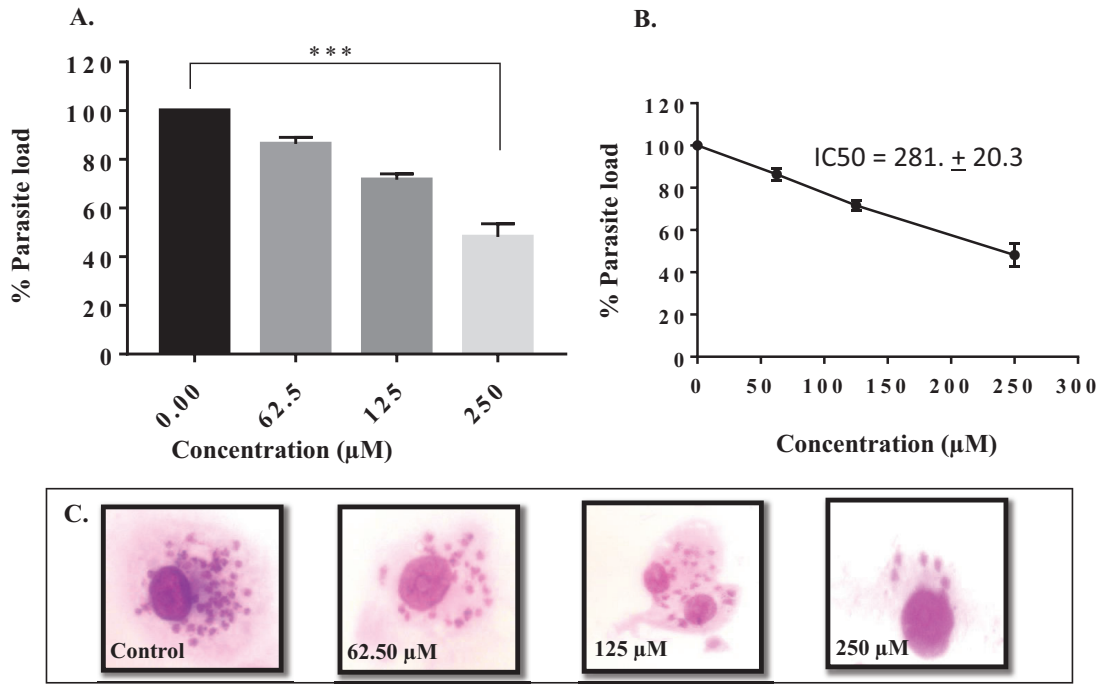


FIGURE 3. Anti-amastigote assay. (A) THP-1 derived macrophages were parasitized as per the method mentioned and parasite load was calculated (B) Extrapolation of Line graph to determine IC 50 value (C) Giemsa-stained micrographs of the infected macrophages at 40 × for visualization of parasites reduction inside macrophages.

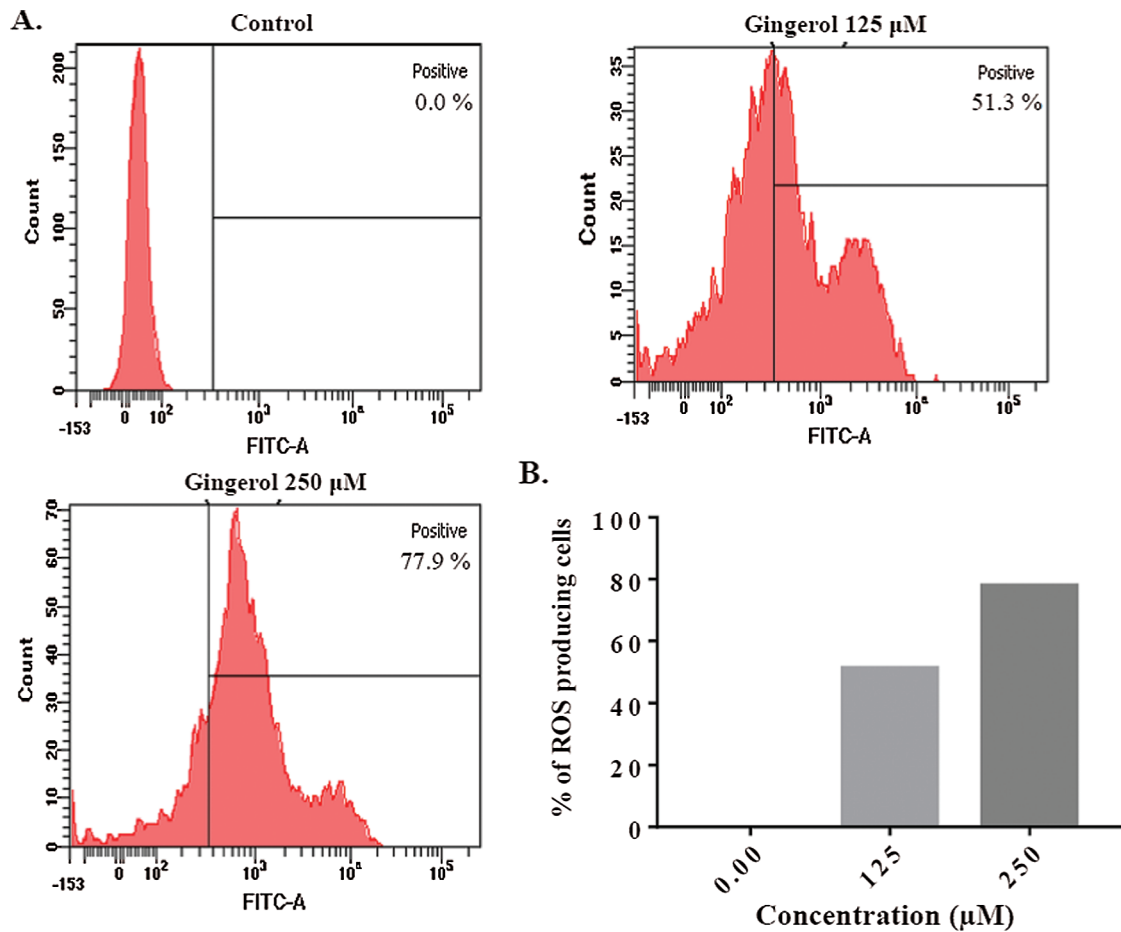


FIGURE 4. Gingerol induced ROS in parasites. For ROS detection 2×10^6 parasites per ml were incubated with 125 µM and 250 µM of gingerol for 48 h. (A) then stained with H2DCFDA dye and parasites were analyzed by flow cytometry. (B) ROS induction by gingerol is shown by bar.

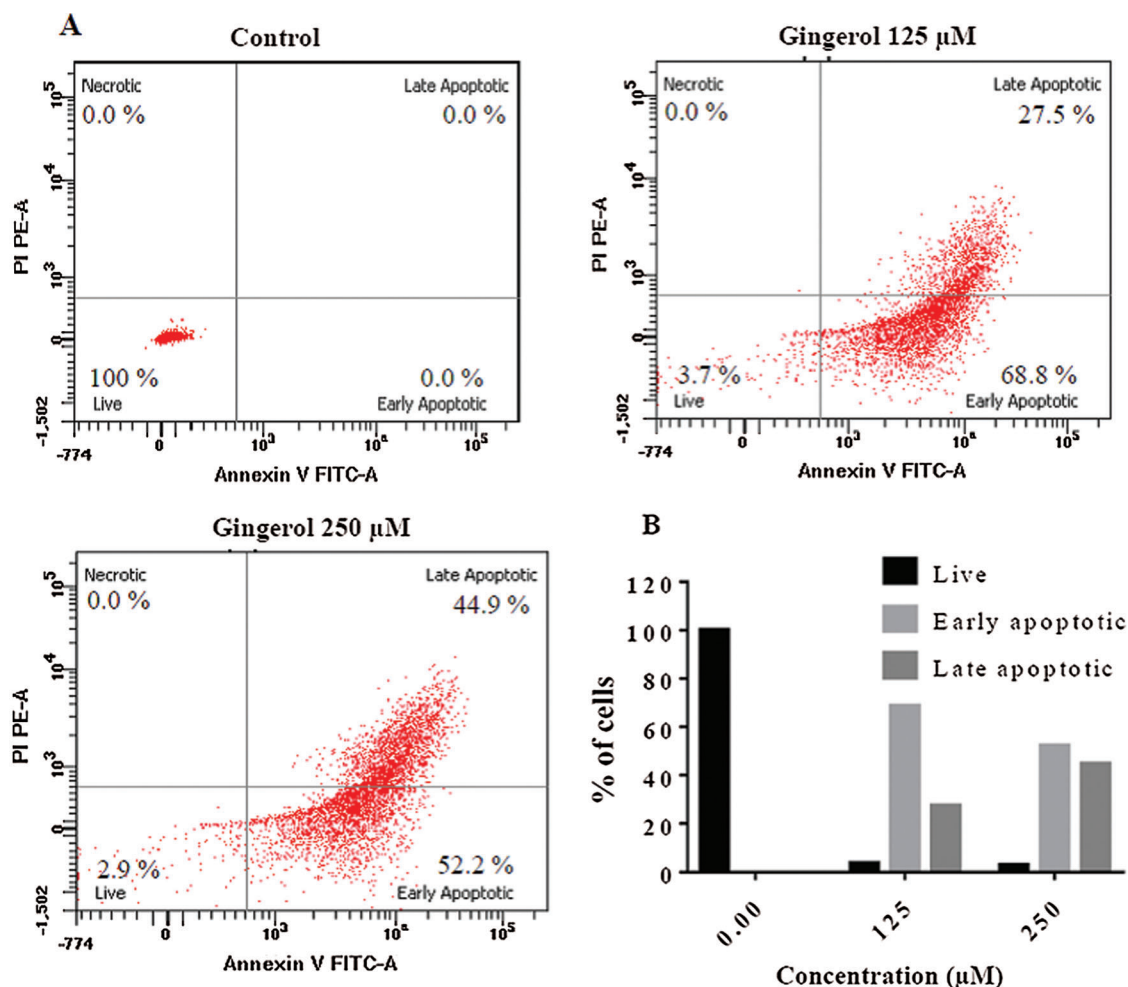


FIGURE 5. Gingerol induced ROS led to apoptosis in parasites. *L. donovani* promastigotes parasites were incubated with 125 μ M and 250 μ M of gingerol for 48 h, followed by (A) staining with Annexin V-FITC/PI and analysis by flow cytometry (B) Bar graph depicts the live, early and late apoptotic cells at the respective concentration of gingerol.

respectively (Tab. 2). We further evaluated their lead likeness and enzyme inhibition activities by exploring ADME properties (Daina et al., 2017) and bioactivity score (<https://www.molinspiration.com/cgi-bin/properties>), gingerol had significant drug-likeness properties (Tab. 4). The interaction of gingerol within the deep cavity of *LdSR* may hinder the substrate accessibility and consequently, may have an inhibitory potential. Gingerol is a phenol phytochemical compound found in fresh ginger. Ginger has been traditionally used for the treatment of illnesses such as common colds and flu, gastrointestinal disturbances, migraines, nausea, asthma, and arthritis (Yusof, 2016). Gingerol has shown a concentration-dependent effect on the logarithmic phase promastigotes, the IC_{50} value of $239.50 \pm 19.26 \mu$ M represents an antileishmanial activity. Additionally, we have done an MTT assay to evaluate the cytotoxic effect of gingerol on the THP-1 differentiated cell line. The cytotoxic effect of gingerol was not lying in the range of leishmanicidal IC_{50} value and was observed in the range of 500 μ M to 1000 μ M. From these values, we can substantiate the safe and potential use of gingerol as a leishmanicidal molecule. The growth of *Mycobacterium* in the lungs, spleen, and liver of mice infected with *Mycobacterium tuberculosis* is restricted upon treatment

with gingerol (Bhaskar et al., 2020). To ascertain the role and effect of gingerol on the internalized amastigotes, we infected the THP-1 differentiated macrophage with *L. donovani* promastigotes and observed a concentration-dependent decrease in the count of amastigotes with an IC_{50} value of $246.90 \pm 17.78 \mu$ M. The IC_{50} values of antipromastigotes and antiamastigotes were found to be approximately in the same range. Gingerol has a nearly equal effect on both promastigotes and amastigotes. Gingerol is reported to have a very prominent anti-cancerous effect and increases the rate of apoptosis and arrest the S-phase stage of the cell cycle thereby inhibiting both the invasive and proliferation capacity of ascites hepatoma AH109A cells (Yagihashi et al., 2008). Gingerol-treated *L. donovani* parasites have shown inhibition by the generation of ROS. ROS generation is an indication of stress condition. With the increasing dose of gingerol, a concentration-dependent increase was detected in the ROS-positive cell. At 125 μ M concentration 51.3% of parasites were observed as ROS positive as compared to control. At 250 μ M concentration, 26.6% and 77.9% of parasites were found to be ROS positive as compared to 125 μ M and control, respectively. Based upon the ROS study, we may infer the pro-oxidant activity of gingerol on *L. donovani*

promastigotes. Generation of ROS leads to apoptosis. With the increasing concentration of gingerol, concentration-dependent increases in apoptotic stages in the parasites have been observed. 96.3% of the parasite population had shown apoptosis by treating the parasite with 125 μ M concentration of gingerol as compared to control. After increasing the dose of gingerol to 250 μ M, the apoptosis was increased to 0.8% and 97.1% as compared to 125 μ M and control, respectively. After increasing the dose from 125 μ M to 250 μ M of gingerol the difference in apoptotic stages was not large but found significant as compared to control. However, based on this data we may infer that the parasites encountered apoptosis on concentration-dependent gingerol treatment.

Our *in-silico* molecular docking-based virtual screening study advocated that gingerol may inhibit *LdSR*, the drug-target of *L. donovani* that plays an important role in their growth and survival. Based on the biological activities of gingerol against different pathological conditions, we aimed to evaluate the potent and effective role of gingerol against leishmaniasis through different *in vitro* experiments. The *in vitro* assays showed the considerable leishmanicidal effect of gingerol against *L. donovani*. Elicited from our results, we may presume the inhibitory potential of gingerol to be treated as a leishmanicidal drug molecule. Further to ascertain the exact mechanism of antileishmanial activity of gingerol, detailed *in vitro* as well as *in vivo* needed.

Acknowledgement: The authors are thankful to the Central Instrumentation facility, Jamia Millia Islamia, New Delhi-110025. We are thankful to Mrs. Nisha Pandey for helping us in making the natural compound library.

Availability of Data and Materials: The data that support the findings of this study are available with the first authors and will be made available upon reasonable request.

Author Contribution: Study was conceptualized, original draft written, edited by AR, SB and AAD; data acquisition and data analysis were performed by ST, RA, SKA, and FR; manuscript preparation and manuscript editing were performed by AR, SB, AAD, FR, BMA, SKA, MAA, MA and ST; the final manuscript was checked by AR, BMA and AAD; fund was obtained by AAD, SB, BMA and AR; Funding acquisition by AR, AAD, SB, MAA, MA; Supervision by AAD, BMA, MAA, MA, SB and AR.

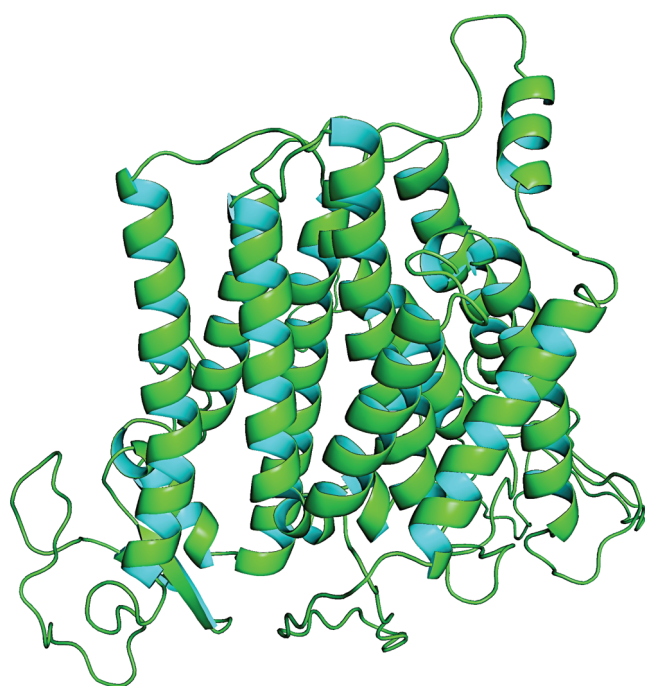
Funding Statement: The Authors would like to thank Deanship of Scientific Research at Majmaah University, Al Majmaah, 11952, Saudi Arabia for supporting this work under the Group Project No. RGP-2019-31.

Conflicts of Interests: The authors declare that they have no conflicts of interest to report regarding the present study.

References

- Abdulhamid A, Awad TA, Ahmed AE, Koua FHM, Ismail AM (2021). Acetylugenol from *Acacia nilotica* (L.) exhibits a strong antibacterial activity and its phenyl and indole analogues show a promising anti-TB potential targeting PknE/B protein kinases. *Microbiology Research* **12**: 1–15.
- Al-Snafi A (2019). A review on *Lawsonia inermis*: A potential medicinal plant. *International Journal of Current Pharmaceutical Research* **11**: 1–13.
- Aronson N, Herwaldt BL, Libman M, Pearson R, Lopez-Velez R, Weina P, Carvalho E, Ephros M, Jeronimo S, Magill A (2017). Diagnosis and treatment of leishmaniasis: Clinical practice guidelines by the Infectious Diseases Society of America (IDSA) and the American Society of Tropical Medicine and Hygiene (ASTMH). *American Journal of Tropical Medicine and Hygiene* **96**: 24–45.
- Bhaskar A, Kumari A, Singh M, Kumar S, Kumar S et al. (2020). [6]-Gingerol exhibits potent anti-mycobacterial and immunomodulatory activity against tuberculosis. *International Immunopharmacology* **87**: 106809.
- Burza S, Croft SL, Boelaert M (2018). Leishmaniasis. *Lancet* **392**: 951–970.
- Cichewicz RH, Thorpe PA (1996). The antimicrobial properties of chile peppers (*Capsicum species*) and their uses in Mayan medicine. *Journal of Ethnopharmacology* **52**: 61–70.
- Cowan MM (1999). Plant products as antimicrobial agents. *Clinical Microbiology Reviews* **12**: 564–582.
- Cheng T, Li Q, Zhou Z, Wang Y, Bryant SH (2012). Structure-based virtual screening for drug discovery: A problem-centric review. *AAPS Journal* **14**: 133–141.
- Dai J, Chen Y, Jiang F (2020). Allicin reduces inflammation by regulating ROS/NLRP3 and autophagy in the context of *A. fumigatus* infection in mice. *Gene* **762**: 145042.
- Daina A, Michielin O, Zoete V (2017). SwissADME: A free web tool to evaluate pharmacokinetics, drug-likeness and medicinal chemistry friendliness of small molecules. *Scientific Reports* **7**: 42717.
- Dallakyan S, Olson AJ (2015). Small-molecule library screening by docking with PyRx. *Methods in Molecular Biology* **1263**: 243–250.
- de Andrade Monteiro C, Ribeiro Alves Dos Santos J (2019). Phytochemicals and their antifungal potential against pathogenic yeasts. *Phytochemicals in Human Health*, 1–31.
- Desjeux P (2004). Leishmaniasis: current situation and new perspectives. *Comparative Immunology, Microbiology and Infectious Diseases* **27**: 305–318.
- Duke J (1987). *CRC Handbook of Medicinal Herbs*. Boca Raton, FL: CRC Press.
- Elmahallawy EK, Sampedro Martinez A, Rodriguez-Granger J, Hoyos-Mallecot Y, Agil A et al. (2014). Diagnosis of leishmaniasis. *Journal of Infection in Developing Countries* **8**: 961–972.
- Ghorbani M, Farhoudi R (2018). Leishmaniasis in humans: Drug or vaccine therapy? *Drug Design Development and Therapy* **12**: 25–40.
- Gilk SD, Beare PA, Heinzen RA (2010). *Coxiella burnetii* expresses a functional $\Delta 24$ sterol reductase. *Journal of Bacteriology* **192**: 6154–6159.
- Goto H, Lauletta Lindoso JA (2012). Cutaneous and mucocutaneous leishmaniasis. *Infectious Disease Clinics* **26**: 293–307.
- Haftom M, Petrucka P, Gemechu K, Nesro J, Amare E et al. (2020). Prevalence and risk factors of human leishmaniasis in Ethiopia: A systematic review and meta-analysis. *Infectious Diseases and Therapy* **10**: 47–60.
- He X, Zhang B, Tan H (2003). Overexpression of a sterol C-24(28) reductase increases ergosterol production in *Saccharomyces cerevisiae*. *Biotechnology Letters* **25**: 773–778.
- Jones Jr, S, Luchsinger A (1986). *Plant Systematic*. New York, NY: McGraw-Hill Book Co.

- Khodavandi A, Harmal NS, Alizadeh F, Scully OJ, Sidik SM et al. (2011). Comparison between allicin and fluconazole in *Candida albicans* biofilm inhibition and in suppression of HWP1 gene expression. *Phytomedicine* **19**: 56–63.
- Kim S (2016). Getting the most out of PubChem for virtual screening. *Expert Opinion in Drug Discovery* **11**: 843–855.
- Lin SC, Ho CT, Chuo WH, Li S, Wang TT, Lin CC (2017). Effective inhibition of MERS-CoV infection by resveratrol. *BMC Infectious Diseases* **17**: 144.
- Maiolini M, Gause S, Taylor J, Steakin T, Shipp G et al. (2020). The war against tuberculosis: A review of natural compounds and their derivatives. *Molecules* **25**: 3011.
- Mathur R, Das RP, Ranjan A, Shaha C (2015). Elevated ergosterol protects *Leishmania* parasites against antimony-generated stress. *FASEB Journal* **29**: 4201–4213.
- Mccall LI, El Aroussi A, Choi JY, Vieira DF, De Muylder G et al. (2015). Targeting ergosterol biosynthesis in *Leishmania donovani*: essentiality of sterol 14 alpha-demethylase. *PLoS Neglected Tropical Diseases* **9**: e0003588.
- O'boyle NM, Banck M, James CA, Morley C, Vandermeersch T, Hutchison GR (2011). Open Babel: An open chemical toolbox. *Journal of Cheminformatics* **3**: 33.
- Palamara AT, Nencioni L, Aquilano K, De Chiara G, Hernandez L et al. (2005). Inhibition of influenza A virus replication by resveratrol. *Journal of Infectious Diseases* **191**: 1719–1729.
- Rahman F, Tabrez S, Ali R, Alqahtani AS, Ahmed MZ, Rub A (2021). Molecular docking analysis of rutin reveals possible inhibition of SARS-CoV-2 vital proteins. *Journal of Traditional and Complementary Medicine* **11**: 173–179.
- Rappé AK, Casewit CJ, Colwell KS, Goddard III, WA, Skiff WM (1992). UFF, a full periodic table force field for molecular mechanics and molecular dynamics simulations. *Journal of the American Chemical Society* **114**: 10024–10035.
- Rollinger JM, Stuppner H, Langer T (2008). Virtual screening for the discovery of bioactive natural products. *Natural Compounds as Drugs Volume 1* **65**: 211–249.
- Simmler C, Antheaume C, Lobstein A (2010). Antioxidant biomarkers from *Vanda coerulea* stems reduce irradiated HaCaT PGE-2 production as a result of COX-2 inhibition. *PLoS One* **5**: e13713.
- Tabrez S, Rahman F, Ali R, Akand SK, Alaidarous MA et al. (2021). Hesperidin targets *Leishmania donovani* sterol C-24 reductase to fight against leishmaniasis. *ACS Omega* **6**: 8112–8118.
- Teodoro AJ (2019). Bioactive compounds of food: Their role in the prevention and treatment of diseases. *Oxidative Medicine and Cellular Longevity* **2019**: 3765986.
- Tian W, Chen C, Lei X, Zhao J, Liang J (2018). CASTp 3.0: Computed atlas of surface topography of proteins. *Nucleic Acids Research* **46**: W363–W367.
- Tiwari N, Gedda MR, Tiwari VK, Singh SP, Singh RK (2018). Limitations of current therapeutic options, possible drug targets and scope of natural products in control of leishmaniasis. *Mini Reviews in Medicinal Chemistry* **18**: 26–41.
- Torres-Guerrero E, Quintanilla-Cedillo MR, Ruiz-Esmenjaud J, Arenas R (2017). Leishmaniasis: A review. *F1000Research* **6**: 750.
- Wild R (1994). *The Complete Book of Natural and Medicinal Cures*. Emmaus, Pa: Rodale Press, Inc.
- Yagihashi S, Miura Y, Yagasaki K (2008). Inhibitory effect of gingerol on the proliferation and invasion of hepatoma cells in culture. *Cytotechnology* **57**: 129–136.
- Yusof YAM (2016). Gingerol and its role in chronic diseases. *Drug Discovery from Mother Nature* **929**: 177–207.
- Zhou L, Wang J, Wang K, Xu J, Zhao J et al. (2012). Chapter 3-Secondary metabolites with antinematodal activity from higher plants. *Studies in Natural Products Chemistry*, vol. 37, pp. 67–114. Elsevier.



SUPPLEMENTARY FIGURE S1. Homology based three-dimensional cartoon representation of *LdSR*.